

B to tensor meson form factors in the perturbative QCD approach

Wei Wang

Istituto Nazionale di Fisica Nucleare, Sezione di Bari, Bari 70126, Italy

We calculate the $B_{u,d,s} \rightarrow T$ form factors within the framework of the perturbative QCD approach, where T denotes a light tensor meson with $J^P = 2^+$. Due to the similarities between the wave functions of a vector and a tensor meson, the factorization formulas of $B \rightarrow T$ form factors can be obtained from the $B \rightarrow V$ transition through a replacement rule. As a consequence, we find that these two sets of form factors have the same signs and correlated q^2 -dependence behaviors. At $q^2 = 0$ point, the $B \rightarrow T$ form factors are smaller than the $B \rightarrow V$ ones, in accordance with the experimental data of radiative B decays. In addition, we use our results for the form factors to explore semileptonic $B \rightarrow Tl\bar{\nu}_l$ decays and the branching fractions can reach the order 10^{-4} .

PACS numbers: 13.20.He; 12.39.St 14.40.Be;

I. INTRODUCTION

In the quark model, a meson is composed of one quark pair and the spin-parity quantum numbers J^P of a meson state is consequently fixed by this constituent quark pair, for instance $J^P = 0^+$ for pseudoscalar mesons. For p-wave tensor mesons with $J^P = 2^+$, both orbital angular momentum L and the total spin S of the quark pair are equal to 1. By making use of the flavor SU(3) symmetry, the nine mesons, isovector mesons $a_2(1320)$, isodoublet states $K_2^*(1430)$ and two isosinglet mesons $f_2(1270)$, $f_2'(1525)$, form the first 3P_2 nonet [1]. These mesons have been well established in various processes.

B meson decays into tensor mesons are of prime interest in several aspects. The main experimental observables in hadronic B decays, branching ratios and CP asymmetries, are helpful to inspect different theoretical computations. One exploration concerns the isospin symmetry. For instance the $B \rightarrow K_2^*(1430)\eta$ channel has already been observed in 2006 with the branching ratio (BR) $(9.1 \pm 3.0) \times 10^{-6}$ for the charged channel and a similar one $(9.6 \pm 2.1) \times 10^{-6}$ for the neutral channel [2]. But the $B \rightarrow \omega K_2^*(1430)$ mode possesses a large isospin violation: the BR for the neutral mode $(10.1 \pm 2.3) \times 10^{-6}$ is about one half of that for the charged mode $(21.5 \pm 4.3) \times 10^{-6}$ [3]. Moreover, polarizations of the final mesons in B decays can shed light on the helicity structure of the electroweak interactions. In the standard model, they are expected to obey a specific hierarchy when factorization is adopted to handle the decay amplitudes and the heavy quark symmetry is exploited to derive relations among the involved form factors. In particular the longitudinal polarization fraction is expected to be close to unity. Deviations from this rule have already been experimentally detected in several B decays to two light vector mesons, with the implication of something beyond the naive expectation. Towards this direction B meson decays into a tensor meson can play a complementary role. For example the decay mode $B \rightarrow \phi K_2^*(1430)$ is mainly dominated by the longitudinal polarization [4, 5], in contrast with the $B \rightarrow \phi K^*$ where the transverse polarization is comparable with the longitudinal one [6].

Despite a number of interesting decay modes have been detected on the experimental side, currently there exist few theoretical investigations on B to tensor transitions. Since a tensor meson can not be produced by a local vector or axial-vector current, the $B \rightarrow MT$ decay amplitude is reduced in terms of the $B \rightarrow T$ transition and the emission of a light meson M . The motif of this work is to handle the first sector with the computation of the $B \rightarrow T$ form factors, and in particular we will use the perturbative QCD (PQCD) approach [7] which is based on the k_T factorization. If the recoiling meson in the final state moves very fast, a hard gluon is required to kick the soft light quark in B meson into an energetic one and then the process is perturbatively calculable. Keeping quarks' intrinsic transverse momentum, the PQCD approach is free of endpoint divergence and the Sudakov formalism makes it more self-consistent. As a direct consequence, we can do the form factor calculation and the quantitative annihilation type diagram calculation in this approach. Our results for these form factors in this work will serve as necessary inputs in the future analysis of the semileptonic and nonleptonic B decays into a tensor meson.

This paper is organized as follows. In Sec. II, we collect the input quantities, including the B -meson wave function, light-cone distribution amplitudes (LCDAs) of light tensor mesons. In Sec. III, we discuss the factorization property of the $B \rightarrow T$ form factors in the PQCD approach. Subsequently we present our numerical results and a comparison with other model predictions is also given. Branching ratios, polarizations and angular asymmetries of the semileptonic $B \rightarrow Tl\bar{\nu}_l$ decays are predicted in Sec. IV. Our summary is given in the last section.

II. WAVE FUNCTIONS

We will work in the B meson rest frame and employ the light-cone coordinates for momentum variables. In the heavy quark limit the light tensor meson in the final state moves very fast in the large-recoil region, we choose its momentum mainly on the plus direction in the light-cone coordinates. The momentum of B meson and the light meson can be written as

$$P_B = \frac{m_B}{\sqrt{2}}(1, 1, 0_\perp), \quad P_2 = \frac{m_B}{\sqrt{2}}(\eta, \frac{r_2^2}{\eta}, 0_\perp), \quad (1)$$

where $r_2 \equiv \frac{m_T}{m_B}$, with m_T, m_B as the mass of the tensor meson and the B meson, respectively. The approximate relation $\eta \approx 1 - q^2/m_B^2$ holds for the momentum transfer $q = P_B - P_2$. The momentum of the light antiquark in B meson and the quark in light mesons are denoted as k_1 and k_2 respectively

$$k_1 = (0, \frac{m_B}{\sqrt{2}}x_1, \mathbf{k}_{1\perp}), \quad k_2 = (\frac{m_B}{\sqrt{2}}x_2\eta, 0, \mathbf{k}_{2\perp}), \quad (2)$$

with x_i being the momentum fraction.

The spin-2 polarization tensor, which satisfies $\epsilon_{\mu\nu}P_2^\nu = 0$, is symmetric and traceless. It can be constructed via the spin-1 polarization vector ϵ :

$$\begin{aligned} \epsilon_{\mu\nu}(\pm 2) &= \epsilon_\mu(\pm)\epsilon_\nu(\pm), \quad \epsilon_{\mu\nu}(\pm 1) = \frac{1}{\sqrt{2}}[\epsilon_\mu(\pm)\epsilon_\nu(0) + \epsilon_\nu(\pm)\epsilon_\mu(0)], \\ \epsilon_{\mu\nu}(0) &= \frac{1}{\sqrt{6}}[\epsilon_\mu(+)\epsilon_\nu(-) + \epsilon_\nu(+)\epsilon_\mu(-)] + \sqrt{\frac{2}{3}}\epsilon_\mu(0)\epsilon_\nu(0). \end{aligned} \quad (3)$$

In the case of the tensor meson moving on the plus direction of the z axis, the explicit structures of ϵ in the ordinary coordinate frame are chosen as

$$\epsilon_\mu(0) = \frac{1}{m_T}(|\vec{p}_T|, 0, 0, E_T), \quad \epsilon_\mu(\pm) = \frac{1}{\sqrt{2}}(0, \mp 1, -i, 0), \quad (4)$$

where E_T and $|\vec{p}_T|$ is the energy and the magnitude of the tensor meson momentum in the B rest frame, respectively. In the following calculation, it is convenient to introduce a new polarization vector ϵ_T for the involved tensor meson

$$\epsilon_{T\mu}(h) = \frac{1}{m_B}\epsilon_{\mu\nu}(h)P_B^\nu, \quad (5)$$

which satisfies

$$\epsilon_{T\mu}(\pm 2) = 0, \quad \epsilon_{T\mu}(\pm 1) = \frac{1}{m_B}\frac{1}{\sqrt{2}}\epsilon(0) \cdot P_B\epsilon_\mu(\pm), \quad \epsilon_{T\mu}(0) = \frac{1}{m_B}\sqrt{\frac{2}{3}}\epsilon(0) \cdot P_B\epsilon_\mu(0). \quad (6)$$

The contraction is evaluated as $\epsilon(0) \cdot P_B/m_B = |\vec{p}_T|/m_T$ and thus we can see that the new vector ϵ_T plays a similar role with the ordinary polarization vector ϵ , regardless of the dimensionless constants $\frac{1}{\sqrt{2}}|\vec{p}_T|/m_T$ or $\sqrt{\frac{2}{3}}|\vec{p}_T|/m_T$.

Tensor meson decay constants are defined through matrix elements of local current operators between the vacuum and a meson state [8]

$$\langle T|j_{\mu\nu}(0)|0\rangle = f_T m_T^2 \epsilon_{\mu\nu}^*, \quad \langle T|j_{\mu\nu\rho}(0)|0\rangle = -if_T^T m_T (\epsilon_{\mu\delta}^* P_{2\nu} - \epsilon_{\nu\delta}^* P_{2\mu}). \quad (7)$$

The interpolating current for f_T is chosen as $j_{\mu\nu} = \frac{1}{2}[\bar{q}_1(0)\gamma_\mu i \overleftrightarrow{D}_\nu q_2(0) + \bar{q}_1(0)\gamma_\nu i \overleftrightarrow{D}_\mu q_2(0)]$ with the covariant derivative $\overleftrightarrow{D}_\nu = \overrightarrow{D}_\nu - \overleftarrow{D}_\nu$: $\overrightarrow{D}_\nu = \partial_\nu + ig_s A_\nu^a \lambda^a/2$ and $\overleftarrow{D}_\nu = \partial_\nu - ig_s A_\nu^a \lambda^a/2$; the one for f_T^\perp is selected as $j_{\mu\nu\rho}^\dagger = \bar{q}_2(0)\sigma_{\mu\nu} i \overleftrightarrow{D}_\delta(0)q_1(0)$. These quantities have been partly calculated in the QCD sum rules in Refs. [9–11] and we quote the recently updated results from Ref. [8] in Tab. I. One interesting feature in these values is that the two decay constants of $a_2(1320)$ are almost equal but large differences are found for $K_2^*(1430)$ and $f_2'(1525)$. In the case of a light vector meson, taking ρ as an example, the transverse decay constant is typically about (20%–30%) smaller than the longitudinal one: $f_\rho^T/f_\rho = (0.687 \pm 0.027)$ [12].

In the PQCD approach, the necessary inputs contain the LCDAs which are constructed by matrix elements of the non-local operators at the light-like separations z_μ with $z^2 = 0$, and sandwiched between the vacuum and the meson

TABLE I: Decay constants of tensor mesons from Ref. [8] (in units of MeV)

f_{a_2}	$f_{a_2}^T$	$f_{K_2^*}$	$f_{K_2^*}^T$	$f_{f_2(1270)}$	$f_{f_2(1270)}^T$	$f_{f_2'(1525)}$	$f_{f_2'(1525)}^T$
107 ± 6	105 ± 21	118 ± 5	77 ± 14	102 ± 6	117 ± 25	126 ± 4	65 ± 12

state. For tensor mesons, their distribution amplitudes are recently analyzed in Ref. [8] which will provide a solid foundation in our study of $B \rightarrow T$ form factors. The LCDAs up to twist-3 for a generic tensor meson are defined by:

$$\begin{aligned} \langle T(P_2, \epsilon) | \bar{q}_{2\beta}(z) q_{1\alpha}(0) | 0 \rangle &= \frac{1}{\sqrt{2N_c}} \int_0^1 dx e^{ixP_2 \cdot z} \left[m_T \not{\epsilon}_{\bullet L}^* \phi_T(x) + \not{\epsilon}_{\bullet L} P_2 \phi_T^t(x) + m_T^2 \frac{\epsilon_{\bullet} \cdot n}{P_2 \cdot n} \phi_T^s(x) \right]_{\alpha\beta}, \\ \langle T(P_2, \epsilon) | \bar{q}_{2\beta}(z) q_{1\alpha}(0) | 0 \rangle &= \frac{1}{\sqrt{2N_c}} \int_0^1 dx e^{ixP_2 \cdot z} \left[m_T \not{\epsilon}_{\bullet T}^* \phi_T^v(x) + \not{\epsilon}_{\bullet T} P_2 \phi_T^T(x) + m_T i \epsilon_{\mu\nu\rho\sigma} \gamma_5 \gamma^\mu \epsilon_{\bullet T}^{*\nu} n^\rho v^\sigma \phi_T^a(x) \right]_{\alpha\beta} \end{aligned} \quad (8)$$

for the longitudinal polarization ($h = 0$) and transverse polarizations ($h = \pm 1$), respectively. Here x is the momentum fraction associated with the q_2 quark. n is the moving direction of the vector meson and v is the opposite direction. $N_c = 3$ is the color factor and the convention $\epsilon^{0123} = 1$ has been adopted. The new vector ϵ_{\bullet} in Eq. (8) is related to the polarization tensor by $\epsilon_{\bullet\mu} \equiv \frac{\epsilon_{\mu\nu} v^\nu}{P_2 \cdot v} m_T = \frac{2\epsilon_{\mu\nu} P_B^\nu}{m_B^2 - q^2} m_T$ and moreover it plays the same role with the polarization vector ϵ in the definition of the vector meson LCDAs. The above distribution amplitudes can be related to the ones given in Ref. [8] by ¹

$$\begin{aligned} \phi_T(x) &= \frac{f_T}{2\sqrt{2N_c}} \phi_{||}(x), & \phi_T^t(x) &= \frac{f_T^t}{2\sqrt{2N_c}} h_{||}^{(t)}(x), \\ \phi_T^s(x) &= \frac{f_T^s}{4\sqrt{2N_c}} \frac{d}{dx} h_{||}^{(s)}(x), & \phi_T^T(x) &= \frac{f_T^T}{2\sqrt{2N_c}} \phi_{\perp}(x), \\ \phi_T^v(x) &= \frac{f_T^v}{2\sqrt{2N_c}} g_{\perp}^{(v)}(x), & \phi_T^a(x) &= \frac{f_T^a}{8\sqrt{2N_c}} \frac{d}{dx} g_{\perp}^{(a)}(x). \end{aligned} \quad (9)$$

The twist-2 LCDA can be expanded in terms of Gegenbauer polynomials $C_n^{3/2}(2x-1)$ weighted by the Gegenbauer moments. Particularly its asymptotic form is

$$\phi_{||,\perp}(x) = 30x(1-x)(2x-1), \quad (10)$$

with the normalization conditions

$$\int_0^1 dx (2x-1) \phi_{||,\perp}(x) = 1. \quad (11)$$

Using equation of motion in QCD, two-particle twist-3 distribution amplitudes are expressed as functions of the twist-2 LCDAs and the three-particle twist-3 LCDAs. In the Wandzura-Wilczek limit, i.e. with the neglect of the three-particle terms, the asymptotic forms of twist-3 LCDAs are derived as [8]

$$h_{||}^{(t)}(x) = \frac{15}{2}(2x-1)(1-6x+6x^2), \quad h_{||}^{(s)}(x) = 15x(1-x)(2x-1), \quad (12)$$

$$g_{\perp}^{(a)}(x) = 20x(1-x)(2x-1), \quad g_{\perp}^{(v)}(x) = 5(2x-1)^3. \quad (13)$$

Since the B meson is a pseudoscalar heavy meson, the two structure $(\gamma^\mu \gamma_5)$ and γ_5 components remain as leading contributions. Then, Φ_B is written by

$$\Phi_B = \frac{i}{\sqrt{6}} \{ (\not{P}_B \gamma_5) \phi_B^A + \gamma_5 \phi_B^P \}, \quad (14)$$

¹ The distribution amplitudes $h_{||}^{(s)}, h_{||}^{(t)}$ and $g_{\perp}^{(v)}$ correspond to h_s, h_t and g_v in Ref. [8], but our $g_{\perp}^{(a)}$ differs from their g_a by a factor of 2: $g_{\perp}^{(a)} = 2g_a$. This definition is more convenient in the following analysis of form factors.

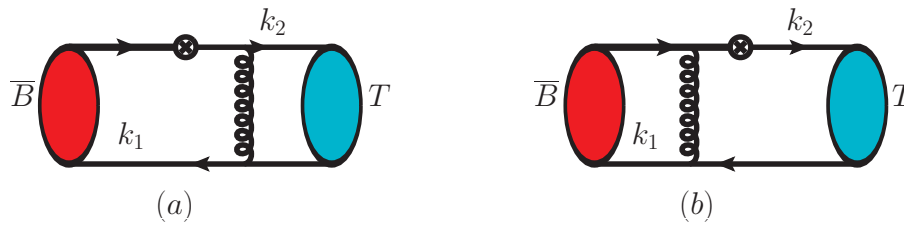


FIG. 1: Feynman diagrams of B meson decays into a tensor meson. The cross represents the weak current, from which a lepton pair can be emitted.

where $\phi_B^{A,P}$ are Lorentz scalar distribution amplitudes. As shown in Ref. [13], B meson's wave function can be simplified into

$$\Phi_B(x, b) = \frac{i}{\sqrt{6}} [(\not{P}_B \gamma_5) + m_B \gamma_5] \phi_B(x, b), \quad (15)$$

where the numerically-suppressed terms in the PQCD approach have been neglected. For the distribution amplitude, we adopt the model:

$$\phi_B(x, b) = N_B x^2 (1-x)^2 \exp \left[-\frac{1}{2} \left(\frac{x m_B}{\omega_B} \right)^2 - \frac{\omega_B^2 b^2}{2} \right], \quad (16)$$

with ω_B being the shape parameter and N_B as the normalization constant. In the above parametrization form, ϕ_B will have a sharp peak at $x \sim 0.1$, in accordance with the most probable momentum fraction of the light quark: Λ_{QCD}/m_B . Here Λ_{QCD} denotes the typical hadronization scale. In recent years, a number of studies of B^\pm and B_d^0 decays have been performed in the PQCD approach, from which the ω_b is found around 0.40 GeV [7, 13]. In our calculation, we will adopt $\omega_b = (0.40 \pm 0.05) \text{ GeV}$ and $f_B = (0.19 \pm 0.02) \text{ GeV}$ for B mesons. For the B_s meson, taking the SU(3) breaking effects into consideration, we employ $\omega_b = (0.50 \pm 0.05) \text{ GeV}$ [14] and $f_{B_s} = (0.23 \pm 0.02) \text{ GeV}$. These values for decay constants are consistent with the recent Lattice QCD simulations [15]

$$f_B = (0.190 \pm 0.01) \text{ GeV}, \quad f_{B_s} = (0.231 \pm 0.015) \text{ GeV}. \quad (17)$$

III. $B \rightarrow T$ FORM FACTORS IN THE PQCD APPROACH

A. PQCD approach

The most important feature of the PQCD approach is that it takes into account the intrinsic transverse momentum of valence quarks. The tree-level transition amplitude, taking the first diagram in Fig. 1 as an example, can be directly expressed as a convolution of wave functions ϕ_B , ϕ_2 and hard scattering kernel T_H with both longitudinal momenta and transverse space coordinates

$$\mathcal{M} = \int_0^1 dx_1 dx_2 \int d^2 \vec{b}_1 d^2 \vec{b}_2 \phi_B(x_1, \vec{b}_1, P_B, t) T_H(x_1, x_2, \vec{b}_1, \vec{b}_2, t) \phi_2(x_2, \vec{b}_2, P_2, t). \quad (18)$$

Individual higher order diagrams may suffer from two generic types of infrared divergences: soft and collinear. In both cases, the loop integration generates logarithmic divergences. These divergences can be separated from the hard kernel and reabsorbed into meson wave functions using eikonal approximation [16]. When soft and collinear momentum overlap, double logarithm divergences will be generated and they can be grouped into the Sudakov factor using the technique of resummation. In the threshold region, loop corrections to the weak decay vertex will also produce double logarithms which can be factored out from the hard part and grouped into the quark jet function. Resummation of the double logarithms results in the threshold factor S_t [17]. This factor decreases faster than any other power of x as $x \rightarrow 0$, which modifies the behavior in the endpoint region to make PQCD approach more self-consistent. For a review of this approach, please see Ref. [18].

With the inclusion of the Sudakov factors, we can get the generic factorization formula in the PQCD approach:

$$\mathcal{M} = \int_0^1 dx_1 dx_2 \int d^2 \vec{b}_1 d^2 \vec{b}_2 \phi_B(x_1, \vec{b}_1, P_B, t) T_H(x_1, x_2, \vec{b}_1, \vec{b}_2, t) \phi_2(x_2, \vec{b}_2, P_2, t) S_t(x_2) \exp[-S_B(t) - S_2(t)]. \quad (19)$$

This factorization framework has been successfully generalized to a number of transition form factors, including different final states such as light pseudoscalar and vector meson [13, 19], scalar mesons [20, 21], axial-vector mesons [22, 23] and the D meson case in large recoil region [24, 25].

B. $B \rightarrow T$ form factors

In analogy with $B \rightarrow V$ form factors, we parameterize the $B \rightarrow T$ form factors as

$$\begin{aligned}
\langle T(P_2, \epsilon) | \bar{q} \gamma^\mu b | \bar{B}(P_B) \rangle &= -\frac{2V(q^2)}{m_B + m_T} \epsilon^{\mu\nu\rho\sigma} \epsilon_{T\nu}^* P_{B\rho} P_{2\sigma}, \\
\langle T(P_2, \epsilon) | \bar{q} \gamma^\mu \gamma_5 b | \bar{B}(P_B) \rangle &= 2im_T A_0(q^2) \frac{\epsilon_T^* \cdot q}{q^2} q^\mu + i(m_B + m_T) A_1(q^2) \left[\epsilon_{T\mu}^* - \frac{\epsilon_T^* \cdot q}{q^2} q^\mu \right] \\
&\quad - i A_2(q^2) \frac{\epsilon_T^* \cdot q}{m_B + m_T} \left[P^\mu - \frac{m_B^2 - m_T^2}{q^2} q^\mu \right], \\
\langle T(P_2, \epsilon) | \bar{q} \sigma^{\mu\nu} q_\nu b | \bar{B}(P_B) \rangle &= -2iT_1(q^2) \epsilon^{\mu\nu\rho\sigma} \epsilon_{T\nu}^* P_{B\rho} P_{2\sigma}, \\
\langle T(P_2, \epsilon) | \bar{q} \sigma^{\mu\nu} \gamma_5 q_\nu b | \bar{B}(P_B) \rangle &= T_2(q^2) [(m_B^2 - m_T^2) \epsilon_{T\mu}^* - \epsilon_T^* \cdot q P^\mu] + T_3(q^2) \epsilon_T^* \cdot q \left[q^\mu - \frac{q^2}{m_B^2 - m_T^2} P^\mu \right], \quad (20)
\end{aligned}$$

where $q = P_B - P_2$, $P = P_B + P_2$. Similar with the $B \rightarrow V$ form factors, we also have the relation $2m_T A_0(0) = (m_B + m_T) A_1(0) - (m_B - m_T) A_2(0)$ for tensor mesons in order to smear the pole at $q^2 = 0$. In the above definitions the flavor factor, for instance $1/\sqrt{2}$ for the isosinglet meson with the component $\frac{1}{\sqrt{2}}(\bar{u}u + \bar{d}d)$, has not been explicitly specified but will be taken into account in the following numerical analysis. The parametrization of $B \rightarrow T$ form factors is analogous to the $B \rightarrow V$ case except that the ϵ is replaced by ϵ_T . In the literature, the $B \rightarrow T$ form factors have been previously defined in an alternative form [26]

$$\begin{aligned}
\langle T(P_2, \epsilon) | V_\mu | \bar{B}(P_B) \rangle &= -h(q^2) \epsilon_{\mu\nu\alpha\beta} \epsilon^{\prime\prime*\nu\lambda} P_\lambda P^\alpha q^\beta, \\
\langle T(P_2, \epsilon) | A_\mu | \bar{B}(P_B) \rangle &= -i \left\{ k(q^2) \epsilon_{\mu\nu}^{\prime\prime*} P^\nu + \epsilon_{\alpha\beta}^{\prime\prime*} P^\alpha P^\beta [P_\mu b_+(q^2) + q_\mu b_-(q^2)] \right\}, \quad (21)
\end{aligned}$$

where the two sets of form factors are related via

$$\begin{aligned}
V &= -m_B(m_B + m_T)h(q^2), \quad A_1 = -\frac{m_B k(q^2)}{m_B + m_T}, \quad A_2 = m_B(m_B + m_T)b_+(q^2), \\
A_0(q^2) &= \frac{m_B + m_T}{2m_T} A_1(q^2) - \frac{m_B - m_T}{2m_T} A_2(q^2) - \frac{m_B q^2}{2m_T} b_-(q^2). \quad (22)
\end{aligned}$$

In the PQCD approach, the factorization formulae of $B \rightarrow T$ form factors can be obtained through a straightforward evaluation of the hard kernels shown in Eq. (19). But the correspondence between a vector meson and a tensor meson allows us to get these formulas in a comparative way. As we have shown in the above, both LCDAs of a tensor meson and the $B \rightarrow T$ form factors are in conjunction with the quantities involving a vector meson and explicitly we have

$$\phi_V^{(i)} \leftrightarrow \phi_T^{(i)}, \quad F^{B \rightarrow T} \leftrightarrow F^{B \rightarrow V}, \quad (23)$$

where $\phi_{V,T}^{(i)}$ and F denotes any generic LCDA and $B \rightarrow (T, V)$ form factor, respectively. The only difference is that the polarization vector ϵ is replaced by ϵ_\bullet in the LCDAs but by ϵ_T in the transition form factors. As a consequence the factorization formulas for the $B \rightarrow T$ form factors are derived as

$$F^{B \rightarrow T}(\phi_T^{(i)}) = \frac{\epsilon_\bullet}{\epsilon_T} F^{B \rightarrow V}(\phi_V^{(i)}) = \frac{2m_B m_T}{m_B^2 - q^2} F^{B \rightarrow V}(\phi_V^{(i)}). \quad (24)$$

As for the expressions of the $B \rightarrow V$ form factors, please see Refs. [13, 19] and also our recent update in Refs. [22, 23].

Form factors in the large recoiling region can be directly calculated since the exchanged gluon is hard enough so that the perturbation theory works well. In order to extrapolate the form factors to the whole kinematic region, we usually use the results obtained in the region $0 < q^2 < 10\text{GeV}^2$ and recast the form factors by adopting certain parametrization of the q^2 -distribution. Unlike the other nonperturbative approaches like the QCD sum rules where the analytic properties can be used to constrain the pole structure of the form factors, the PQCD approach is mainly established on the perturbative property of the form factors (i.e. factorization) and in this approach one has to assume

the parametrization form in a phenomenological way. In the literature, the popular forms for $B \rightarrow P$ and $B \rightarrow V$ form factors (P, V denotes a light pseudoscalar meson and a vector meson respectively) include pole form, dipole form and exponential form, and the BK parametrization [27]. In the small q^2 region, these forms do not differ too much as all of them have similar forms by making use of the expansion of q^2/m_B^2 . Unfortunately the differences increase with the increase of q^2 . The limited knowledge of the form factors in the large q^2 region will inevitably introduce sizable uncertainties. However as a first step to proceed, it is helpful to investigate these form factors by employing one commonly-adopted form. The dipole form has been adopted in the previous PQCD studies [21–23]

$$F(q^2) = \frac{F(0)}{1 - a(q^2/m_B^2) + b(q^2/m_B^2)^2} \quad (25)$$

and this parametrization works well. In contrast, the $B \rightarrow T$ form factors receive additional q^2 -dependence as can be seen from the factorization formulas in Eq. (24). In this case the following modified form is more appropriate for the q^2 -distribution of $B \rightarrow T$ form factors

$$F(q^2) = \frac{F(0)}{(1 - q^2/m_B^2)(1 - a(q^2/m_B^2) + b(q^2/m_B^2)^2)}, \quad (26)$$

and we shall use this form in our fitting procedure.

Numerical results for the form factors at maximally recoil point and the two fitted parameters a, b are collected in table II. The first type of errors comes from decay constants and shape parameter ω_b of B meson; while the second one is from factorization scales (from $0.75t$ to $1.25t$, not changing the transverse part $1/b_i$), the threshold resummation parameter $c = 0.4 \pm 0.1$ and $\Lambda_{\text{QCD}} = (0.25 \pm 0.05)\text{GeV}$. The hadron masses are taken from particle data group [1]

$$m_{a_2} = 1.3183\text{GeV}, \quad m_{K_2^*} = 1.43\text{GeV}, \quad m_{f_2(1270)} = 1.2751\text{GeV}, \quad m_{f_2'(1525)} = 1.525\text{GeV}. \quad (27)$$

A number of remarks on these results are given in order.

1. With terms suppressed by r_2^2 neglected, $A_2(q^2)$ can be expressed as a linear combination of A_0 and A_1 [23]

$$A_2(q^2) = \frac{1 + r_2}{1 - q^2/m_B^2} [(1 + r_2)A_1(q^2) - 2r_2A_0(q^2)]. \quad (28)$$

We will use this relation for $A_2(q^2)$ in the whole kinematic region instead of a direct fitting.

2. The $B \rightarrow f_2(1270)$ form factors are smaller than the other channels due to the factor $1/\sqrt{2}$ in the flavor wave function of $f_2(1270)$. The smaller transverse decay constants of K_2^* and $f_2'(1525)$ have a tendency to suppress the transition amplitudes. But their larger masses give an enhancement, since both contributions from the twist-3 LCDAs and the correspondence relation in Eq. (24) are proportional to the hadron mass.
3. The parameters a in most transition form factors are roughly 1.7, but they are around 0.7 for $A_1(q^2)$ and $T_2(q^2)$. Analogously the parameter b is close to 0.6 with the exception for $A_1(q^2)$ and $T_2(q^2)$ as it is approaching 0. The vanishing b implies that the dipole behavior in these two form factors is reduced into the monopole form.
4. In our computation, the asymptotic forms for the LCDAs have been adopted. The twist-2 LCDAs $\phi_{\parallel, \perp}$ can be expanded into Gegenbauer polynomials $C_n^{3/2}(2x_2 - 1)$ (with x_2 being the momentum fraction of the quark in the meson) and the twist-3 LCDAs will be expressed in terms of twist-2 ones through the use of equation of motion [8]:

$$\begin{aligned} g_{\perp}^{(v)}(x_2) &= \int_0^{x_2} dv \frac{\phi_{\parallel}(v)}{1-v} + \int_{x_2}^1 dv \frac{\phi_{\parallel}(v)}{v}, \\ g_{\perp}^{(a)}(x_2) &= 4(1-x_2) \int_0^{x_2} dv \frac{\phi_{\parallel}(v)}{1-v} + 4x_2 \int_{x_2}^1 dv \frac{\phi_{\parallel}(v)}{v}, \\ h_{\parallel}^{(t)}(x_2) &= \frac{3}{2}(2x_2-1) \left[\int_0^{x_2} dv \frac{\phi_{\perp}(v)}{1-v} - \int_{x_2}^1 dv \frac{\phi_{\perp}(v)}{v} \right], \\ h_{\parallel}^{(s)}(x_2) &= 3(1-x_2) \int_0^{x_2} dv \frac{\phi_{\perp}(v)}{1-v} + 3x_2 \int_{x_2}^1 dv \frac{\phi_{\perp}(v)}{v}. \end{aligned} \quad (29)$$

TABLE II: $B \rightarrow T$ form factors. a, b are the parameters of the form factors in the parametrization shown in Eq. (26). The two kinds of errors are from: decay constants of B meson and shape parameter ω_b ; Λ_{QCD} , the scales ts and the threshold resummation parameter c .

F	$F(0)$	a	b	F	$F(0)$	a	b
V^{Ba_2}	$0.18^{+0.04+0.04}_{-0.03-0.03}$	$1.70^{+0.01+0.06}_{-0.01-0.05}$	$0.63^{+0.03+0.09}_{-0.01-0.04}$	$V^{Bf_2(1270)}$	$0.12^{+0.02+0.02}_{-0.02-0.02}$	$1.68^{+0.02+0.06}_{-0.00-0.05}$	$0.62^{+0.05+0.10}_{-0.00-0.07}$
$A_0^{Ba_2}$	$0.18^{+0.04+0.04}_{-0.03-0.03}$	$1.74^{+0.00+0.06}_{-0.05-0.07}$	$0.71^{+0.00+0.07}_{-0.13-0.13}$	$A_0^{Bf_2(1270)}$	$0.13^{+0.03+0.03}_{-0.02-0.02}$	$1.74^{+0.01+0.05}_{-0.02-0.06}$	$0.69^{+0.04+0.06}_{-0.05-0.10}$
$A_1^{Ba_2}$	$0.11^{+0.02+0.02}_{-0.02-0.02}$	$0.74^{+0.02+0.04}_{-0.01-0.03}$	$-0.11^{+0.04+0.03}_{-0.03-0.02}$	$A_1^{Bf_2(1270)}$	$0.08^{+0.02+0.01}_{-0.01-0.01}$	$0.73^{+0.01+0.05}_{-0.03-0.04}$	$-0.12^{+0.03+0.04}_{-0.09-0.00}$
$A_2^{Ba_2}$	$0.06^{+0.01+0.01}_{-0.01-0.01}$	--	--	$A_2^{Bf_2(1270)}$	$0.04^{+0.01+0.01}_{-0.01-0.00}$	--	--
$T_1^{Ba_2}$	$0.15^{+0.03+0.03}_{-0.03-0.02}$	$1.69^{+0.00+0.05}_{-0.01-0.05}$	$0.64^{+0.00+0.05}_{-0.04-0.06}$	$T_1^{Bf_2(1270)}$	$0.10^{+0.02+0.02}_{-0.02-0.01}$	$1.67^{+0.00+0.05}_{-0.01-0.08}$	$0.62^{+0.00+0.05}_{-0.03-0.15}$
$T_2^{Ba_2}$	$0.15^{+0.03+0.03}_{-0.03-0.02}$	$0.74^{+0.01+0.01}_{-0.01-0.07}$	$-0.11^{+0.02+0.00}_{-0.01-0.09}$	$T_2^{Bf_2(1270)}$	$0.10^{+0.02+0.02}_{-0.02-0.01}$	$0.72^{+0.00+0.03}_{-0.04-0.08}$	$-0.09^{+0.00+0.00}_{-0.10-0.11}$
$T_3^{Ba_2}$	$0.13^{+0.03+0.03}_{-0.02-0.02}$	$1.58^{+0.01+0.06}_{-0.01-0.05}$	$0.52^{+0.02+0.05}_{-0.04-0.04}$	$T_3^{Bf_2(1270)}$	$0.09^{+0.02+0.02}_{-0.02-0.01}$	$1.56^{+0.03+0.08}_{-0.00-0.05}$	$0.48^{+0.08+0.12}_{-0.00-0.04}$
$V^{BK_2^*}$	$0.21^{+0.04+0.05}_{-0.04-0.03}$	$1.73^{+0.02+0.05}_{-0.02-0.03}$	$0.66^{+0.04+0.07}_{-0.05-0.01}$				
$A_0^{BK_2^*}$	$0.18^{+0.04+0.04}_{-0.03-0.03}$	$1.70^{+0.00+0.05}_{-0.02-0.07}$	$0.64^{+0.00+0.04}_{-0.06-0.10}$				
$A_1^{BK_2^*}$	$0.13^{+0.03+0.03}_{-0.02-0.02}$	$0.78^{+0.01+0.05}_{-0.01-0.04}$	$-0.11^{+0.02+0.04}_{-0.03-0.02}$				
$A_2^{BK_2^*}$	$0.08^{+0.02+0.02}_{-0.02-0.01}$	--	--				
$T_1^{BK_2^*}$	$0.17^{+0.04+0.04}_{-0.03-0.03}$	$1.73^{+0.00+0.05}_{-0.03-0.07}$	$0.69^{+0.00+0.05}_{-0.08-0.11}$				
$T_2^{BK_2^*}$	$0.17^{+0.03+0.04}_{-0.03-0.03}$	$0.79^{+0.00+0.02}_{-0.04-0.09}$	$-0.06^{+0.00+0.00}_{-0.10-0.16}$				
$T_3^{BK_2^*}$	$0.14^{+0.03+0.03}_{-0.03-0.02}$	$1.61^{+0.01+0.09}_{-0.00-0.04}$	$0.52^{+0.05+0.15}_{-0.01-0.01}$				
$V^{B_s K_2^*}$	$0.18^{+0.03+0.04}_{-0.03-0.03}$	$1.73^{+0.02+0.05}_{-0.00-0.05}$	$0.67^{+0.05+0.06}_{-0.00-0.05}$	$V^{B_s f_2'(1525)}$	$0.20^{+0.04+0.05}_{-0.03-0.03}$	$1.75^{+0.02+0.05}_{-0.00-0.03}$	$0.69^{+0.05+0.08}_{-0.01-0.01}$
$A_0^{B_s K_2^*}$	$0.15^{+0.03+0.03}_{-0.02-0.02}$	$1.70^{+0.00+0.03}_{-0.01-0.05}$	$0.65^{+0.01+0.00}_{-0.03-0.04}$	$A_0^{B_s f_2'(1525)}$	$0.16^{+0.03+0.03}_{-0.02-0.02}$	$1.69^{+0.00+0.04}_{-0.01-0.03}$	$0.64^{+0.00+0.01}_{-0.04-0.02}$
$A_1^{B_s K_2^*}$	$0.11^{+0.02+0.02}_{-0.02-0.02}$	$0.79^{+0.02+0.03}_{-0.01-0.03}$	$-0.10^{+0.07+0.06}_{-0.03-0.02}$	$A_1^{B_s f_2'(1525)}$	$0.12^{+0.02+0.03}_{-0.02-0.02}$	$0.80^{+0.02+0.07}_{-0.00-0.03}$	$-0.11^{+0.05+0.09}_{-0.00-0.00}$
$A_2^{B_s K_2^*}$	$0.07^{+0.01+0.02}_{-0.01-0.01}$	--	--	$A_2^{B_s f_2'(1525)}$	$0.09^{+0.02+0.02}_{-0.01-0.01}$	--	--
$T_1^{B_s K_2^*}$	$0.15^{+0.03+0.03}_{-0.02-0.02}$	$1.73^{+0.00+0.04}_{-0.01-0.06}$	$0.69^{+0.00+0.04}_{-0.03-0.11}$	$T_1^{B_s f_2'(1525)}$	$0.16^{+0.03+0.04}_{-0.03-0.02}$	$1.75^{+0.01+0.05}_{-0.00-0.05}$	$0.71^{+0.03+0.06}_{-0.01-0.08}$
$T_2^{B_s K_2^*}$	$0.15^{+0.03+0.03}_{-0.02-0.02}$	$0.80^{+0.00+0.02}_{-0.03-0.08}$	$-0.06^{+0.00+0.00}_{-0.09-0.13}$	$T_2^{B_s f_2'(1525)}$	$0.16^{+0.03+0.04}_{-0.03-0.02}$	$0.82^{+0.00+0.04}_{-0.04-0.06}$	$-0.08^{+0.00+0.03}_{-0.09-0.08}$
$T_3^{B_s K_2^*}$	$0.12^{+0.02+0.03}_{-0.02-0.02}$	$1.61^{+0.03+0.08}_{-0.00-0.04}$	$0.52^{+0.08+0.14}_{-0.01-0.00}$	$T_3^{B_s f_2'(1525)}$	$0.13^{+0.03+0.03}_{-0.02-0.02}$	$1.64^{+0.02+0.06}_{-0.00-0.06}$	$0.57^{+0.04+0.05}_{-0.01-0.09}$

Taking into account the contributions from the next non-zero Gegenbauer moment besides the asymptotic form, i.e. a_3 , we find

$$A_0^{Ba_2}(0) = 0.18 \pm 0.07a_3, \quad T_1^{Ba_2}(0) = 0.15 \pm 0.057a_3. \quad (30)$$

In the case of π and ρ meson, the first non-zero Gegenbauer moment is around (0.2-0.3) [28]. If it were the similar for the tensor meson, we can see that the form factors will be changed by roughly 10% – 20%.

- Since the $B \rightarrow T$ form factors are obtained from the $B \rightarrow V$ ones, it is meaningful to analyze these two sets of form factors in a comparative way. It is worth comparing their distribution amplitudes. The six LCDAs are functions of x_2 , with x_2 being the momentum fraction of the quark in the light meson. Taking ρ and a_2 mesons as an example, these LCDAs are depicted in Fig. 2, where the solid (dashed) lines denote the LCDAs for ρ (a_2) meson. For ρ meson LCDAs, the asymptotic form has been used. From this figure, we can see that although the two sets of LCDAs are different in the small-momentum-fraction region $x_2 < 0.5$, they have similar shapes when $x_2 > 0.6$. The large-momentum-fraction region, $0.6 < x_2 < 1$ ² dominates in the PQCD approach. As one

² The dominant region in the PQCD approach can be obtained by the power counting in this approach which has been established in Ref. [29]. The typical momentum of the spectator (with the momentum fraction $1 - x_2$) is of the order $\Lambda/m_B < 0.3$ with the vary of the hadronization scale Λ . This means that the dominant contribution lies in the region of $0.7 < x_2$. This conclusion can also be drawn in a simple way. PQCD is based on the hard scattering picture, in which the endpoint region $x_2 \sim 0, 1$ is suppressed by the Sudakov factor. In the Feynman diagrams given in Fig.1, if the momentum of the spectator (with momentum fraction $1 - x_2$) is getting larger, the gluon and the quark propagators will have larger virtualities. For instance, they are $p_b^2 - m_b^2 = x_2 \eta m_B^2 - k_{1\perp}^2$ and $p_g^2 = x_1 x_2 \eta m_B^2 - (k_{1\perp} - k_{2\perp})^2$ with the transverse component $k_{1\perp, 2\perp}$ of the order Λ . Therefore the region $x_2 > 0.5$ is more important compared with the region of $x_2 < 0.5$ and thus in our analysis the region of $x_2 > 0.6$ is chosen.

TABLE III: $B \rightarrow \rho$ form factors in the PQCD approach [23]

F	$F(0)$	a	b
V	$0.21^{+0.05+0.03}_{-0.04-0.02}$	1.75	0.69
A_0	$0.25^{+0.06+0.04}_{-0.05-0.03}$	1.69	0.57
A_1	$0.16^{+0.04+0.02}_{-0.03-0.02}$	0.77	-0.13
A_2	$0.13^{+0.03+0.02}_{-0.03-0.01}$	—	—
T_1	$0.19^{+0.04+0.03}_{-0.04-0.02}$	1.69	0.61
T_2	$0.19^{+0.04+0.03}_{-0.04-0.02}$	0.73	-0.12
T_3	$0.17^{+0.04+0.02}_{-0.03-0.02}$	1.58	0.50

TABLE IV: Different contributions to form factors A_0 and T_1 for $B \rightarrow \rho$ and $B \rightarrow a_2(1320)$.

A_0	$B \rightarrow \rho$	$B \rightarrow a_2(1320)$
ϕ	0.108	0.050
ϕ^s	0.103	0.088
ϕ^t	0.040	0.046
total	0.251	0.184
T_1	$B \rightarrow \rho$	$B \rightarrow a_2(1320)$
ϕ^T	0.085	0.049
ϕ^a	0.047	0.046
ϕ^v	0.063	0.054
total	0.194	0.150

important consequence, the $B \rightarrow T$ and $B \rightarrow V$ form factors will have several similar properties. For instance the two kinds of form factors will have the same signs and their q^2 -dependence parameters will also be close.

- As functions of q^2 , the $B \rightarrow T$ form factors are expected to be sharper than the $B \rightarrow V$ form factors, since the former ones contain one more pole structure in the q^2 -distribution. To illustrate this situation, in Fig. 3 we show the $B \rightarrow \rho$ (dashed lines) and $B \rightarrow a_2$ form factors (solid lines) in the region of $0 < q^2 < 10\text{GeV}^2$, where the PQCD results for the $B \rightarrow \rho$ form factors are taken from our recent update in Ref. [23]. We also quote them in table III, but only the central values are shown for the q^2 -dependence parameters a, b . The ratio of the $B \rightarrow \rho$ and $B \rightarrow a_2$ form factors is 0.73 for A_0 and 0.77 for T_1 , respectively.
- At the maximally recoiling point with $q^2 = 0$, the $B \rightarrow \rho$ and $B \rightarrow a_2(1320)$ form factors have different magnitudes. Taking A_0 and T_1 as an example, in table IV we enumerate distinct contributions from the three LCDAs. The matching coefficient $2m_T m_B / (m_B^2 - q^2)$ between the two sets of form factors is roughly 1/2 at $q^2 = 0$ and in this case the $B \rightarrow T$ transition is expected to be smaller. It is also confirmed by the numerical results in table IV, where its twist-2 contribution is only one half of the $B \rightarrow V$ case. On the contrary this does not occur for the twist-3 LCDAs, as the larger tensor meson mass has compensated the suppression: $m_{a_2} \sim 2m_\rho$.

In the literature, the $B \rightarrow T$ form factors have been explored in the ISGW model [26], its improved form ISGW II model [30–33] and other relativistic quark models for instance the covariant light-front quark model (LFQM) [34–36]. The form factor T_1 for $B \rightarrow K_2^*$ is also estimated in the technique of QCD sum rules (QCDSR) [37], relativistic quark model [38] and heavy quark symmetry [39]. We collect the results using these approaches [32–37] in table V for the convenience of a comparison, where their results have been converted to the new form factors defined in Eq. (20) through the relations in Eq. (22). Our PQCD results, all uncertainties added in quadrature, are also shown in table V. From this table, we can find many differences among these theoretical predictions. Results for all form factors from the ISGW II model possess a different sign with our results and the magnitudes are typically larger. The two calculations in the same ISGW II model are also different, for instance the prediction in Ref. [32] of A_2 for $B \rightarrow K_2^*$ is about twice as large as the one in Ref. [33]. The estimate in the QCDSR [37] is consistent with our result.

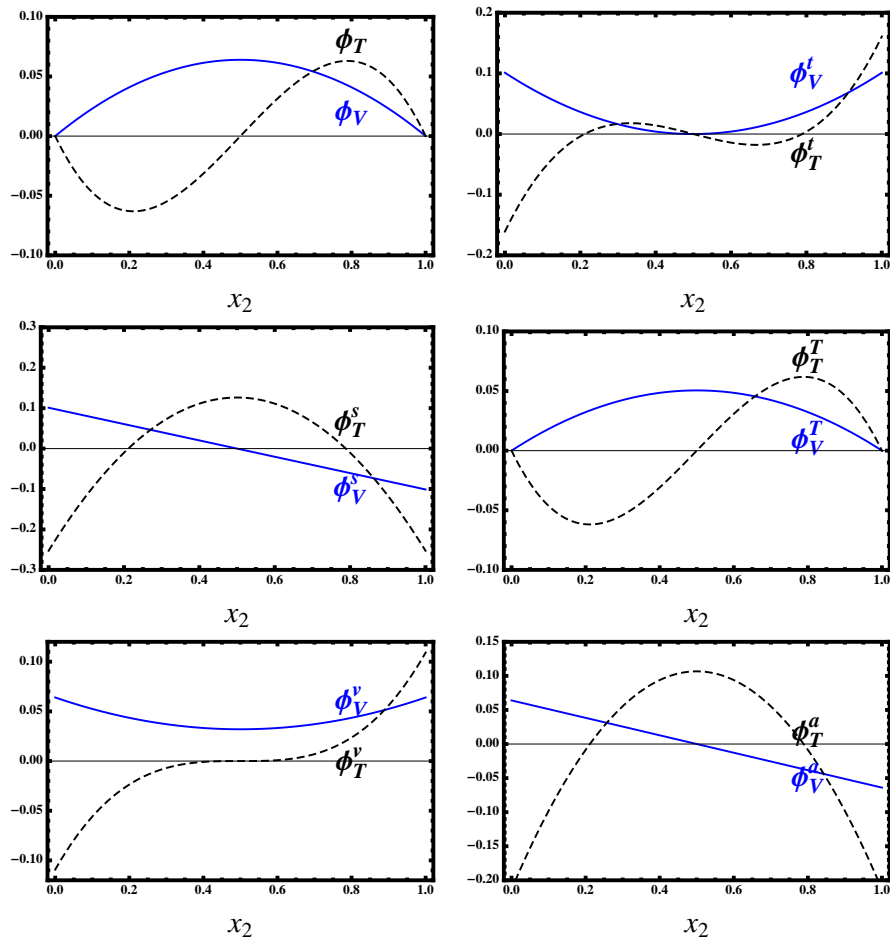


FIG. 2: LCDAs of the vector meson ρ (solid lines) and its tensor counterpart a_2 (dashed lines). The asymptotic forms are adopted for ρ, a_2 meson LCDAs.

Results in the covariant LFQM are different with ours in several aspects. Firstly, for A_0 and $T_{1,2}$ ³, the LFQM predicts the same sign with our results but the remanent results have negative signs. Secondly, their predictions, except for A_1 , are much larger than ours in magnitude. Moreover the q^2 -distribution is also different. In Fig. 3, we show the LFQM results (dotted lines) in the region of $0 < q^2 < 10\text{GeV}^2$, with $V, A_{0,1,2}$ for the $B \rightarrow a_2$ process [34] but $T_{1,2,3}$ for the $B \rightarrow K_2^*$ transition [36]. A minus sign has been added to V, A_1, A_2, T_3 so that they have the same sign with our results. From this figure, we can find that the differences for A_1, A_2, T_2 between their results and ours get larger as q^2 grows. In particular, the T_2 grows faster than T_1 with the increase of q^2 in the LFQM but it is reverse in our results. In the covariant LFQM the meson-quark-antiquark coupling vertex for a tensor meson contains $\epsilon_{\mu\nu} \frac{p_1^\nu - p_2^\nu}{2} \sqrt{\frac{2}{\beta'^2}}$, which corresponds to ϵ_μ in the case of a vector meson. $p_1'(p_2)$ denotes the momentum of the quark and antiquark in the final meson. The β' , of the order Λ_{QCD} , is the shape parameter which characterizes the momentum distribution inside the tensor meson. It is hard to deduce the relative signs from this structure since (1) apart from the longitudinal momentum in p_1', p_2 , the transverse part might also contribute; (2) it involves the zero-mode terms which are essential for the maintenance of the Lorentz covariance. In this sense the relation between a vector meson and its tensor counterpart is not as simple as the one in the PQCD approach, where ϵ is replaced by ϵ_\bullet . These different results can be discriminated in the future when enough data is available.

In the large energy limit, the seven $B \rightarrow T$ form factors are expected to satisfy several nontrivial relations [40, 41] and all form factors can be parameterized into two independent functions $\zeta_\perp(q^2)$ and $\zeta_\parallel(q^2)$. In the large recoil region, we have checked that our results respect these relations. Moreover, the relative size of these two functions is also of

³ The form factors $T_{1,2,3}$ in this work correspond to the $U_{1,2,3}$ in Ref. [36].

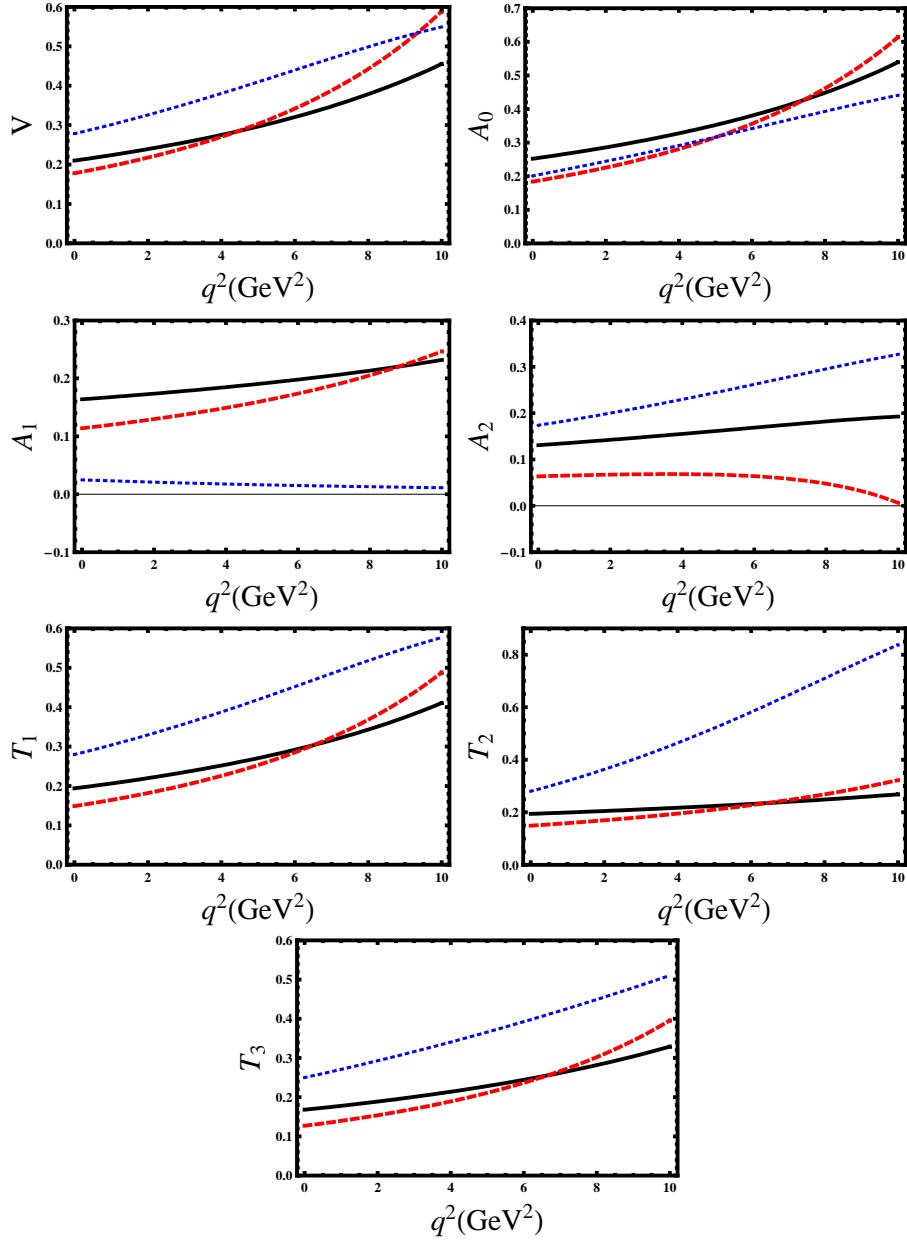


FIG. 3: Transition form factors as functions of q^2 . Solid (black) and dashed (red) lines correspond to our results of the $B \rightarrow \rho$ and $B \rightarrow a_2$ channel, respectively. Dotted (blue) lines denote the results in the covariant LFQM, with V, A_0, A_1, A_2 for the $B \rightarrow a_2$ process and $T_{1,2,3}$ for the $B \rightarrow K_2^*$ transition. A minus sign has been added to the LFQM results for V, A_1, A_2, T_3 so that they have the same sign with our results.

prime interest but it can not be deduced from the large energy limit itself. Our results for the $B \rightarrow K_2^*$ transition ⁴,

$$\zeta_{\perp}(0) = \frac{|\vec{p}_{K_2^*}|}{m_{K_2^*}} T_1^{BK_2^*}(0) = (0.29 \pm 0.09), \quad \zeta_{\parallel}(0) = \frac{1}{1 - \frac{m_{K_2^*}^2}{m_B E_{K_2^*}}} \left(\frac{|\vec{p}_{K_2^*}|}{m_{K_2^*}} A_0^{BK_2^*}(0) - \frac{m_{K_2^*}}{m_B} \zeta_{\perp}(0) \right) = (0.26 \pm 0.10),$$

show that they are of similar size, the same conclusion with the $B \rightarrow V$ cases. This is not accidental but instead is an outcome of the similar shapes between the vector and tensor meson LCDAs in the dominant region of the PQCD

⁴ We use the definitions of ζ_{\perp} and ζ_{\parallel} in Ref. [41], but our form factors correspond to theirs with a tilde.

TABLE V: $B \rightarrow T$ form factors at maximally recoil, i.e. $q^2 = 0$. Theoretical results in the ISGW II model [32], the covariant light-front quark model [34, 36] and the QCD sum rules [37] are also collected for a comparison. Results in the parentheses are from Ref. [33].

		$B \rightarrow a_2$	$B \rightarrow K_2^*$	$B \rightarrow f_2$	$B_s \rightarrow K_2^*$	$B_s \rightarrow f_2'$
ISGW II [32]([33])	V		$-(0.57)$			
	A_0	-0.18	-0.17(-0.25)	-0.08	-0.27	-0.26
	A_1	-0.35	-0.38(-0.23)	-0.24	-0.39	-0.45
	A_2	-0.45	-0.53(-0.21)	-0.34	-0.47	-0.59
LFQM [34, 36]	V	-0.28	-0.28			
	A_0	0.20	0.26			
	A_1	-0.025	-0.012			
	A_2	-0.17	-0.21			
	$T_1 = T_2$		0.28			0.28
	T_3		-0.25			-0.18
QCDSR [37]	T_1		0.19 ± 0.04			
This work	V	$0.18^{+0.05}_{-0.04}$	$0.21^{+0.06}_{-0.05}$	$0.12^{+0.03}_{-0.03}$	$0.18^{+0.05}_{-0.04}$	$0.20^{+0.06}_{-0.04}$
	A_0	$0.18^{+0.06}_{-0.04}$	$0.18^{+0.05}_{-0.04}$	$0.13^{+0.04}_{-0.03}$	$0.15^{+0.04}_{-0.03}$	$0.16^{+0.04}_{-0.03}$
	A_1	$0.11^{+0.03}_{-0.03}$	$0.13^{+0.04}_{-0.03}$	$0.08^{+0.02}_{-0.02}$	$0.11^{+0.03}_{-0.02}$	$0.12^{+0.03}_{-0.03}$
	A_2	$0.06^{+0.02}_{-0.01}$	$0.08^{+0.03}_{-0.02}$	$0.04^{+0.01}_{-0.01}$	$0.07^{+0.02}_{-0.02}$	$0.09^{+0.03}_{-0.02}$
	$T_1 = T_2$	$0.15^{+0.04}_{-0.03}$	$0.17^{+0.05}_{-0.04}$	$0.10^{+0.03}_{-0.02}$	$0.15^{+0.04}_{-0.03}$	$0.16^{+0.05}_{-0.04}$
	T_3	$0.13^{+0.04}_{-0.03}$	$0.14^{+0.05}_{-0.03}$	$0.09^{+0.03}_{-0.02}$	$0.12^{+0.04}_{-0.03}$	$0.13^{+0.04}_{-0.03}$

approach. Our result is also accordance with the theoretical estimate in Ref. [41]

$$\zeta_{\perp}(0) = 0.27 \pm 0.03^{+0.00}_{-0.01}. \quad (31)$$

On the experimental side the branching ratio of the color-allowed tree-dominated processes $B^0 \rightarrow a_2^{\pm} \pi^{\mp}$ has been set with an upper limit

$$\mathcal{B}(B^0 \rightarrow a_2^{\pm} \pi^{\mp}) < 3.0 \times 10^{-4}. \quad (32)$$

When factorization is adopted this mode can be used to extract the $B \rightarrow a_2$ form factor

$$|A_0^{B \rightarrow a_2}(q^2 = 0)| < 7.6 F_+^{B \rightarrow \pi}(q^2 = 0) \simeq 1.9, \quad (33)$$

where penguin contributions have been neglected as a result of their small Wilson coefficients. Unfortunately the above constraint is too loose to provide any useful information on the characters of the tensor mesons. We expect more news on this front from the B factories and other experiment facilities, including the Large Hadron Collider.

At the leading order of α_s , both $B \rightarrow K^* \gamma$ and $B \rightarrow K_2^* \gamma$ only receive contributions from the chromo-magnetic operator $O_{7\gamma}$, which leads to

$$\begin{aligned} \mathcal{B}(B \rightarrow K^* \gamma) &= \tau_B \frac{G_F^2 \alpha_{\text{em}} m_B^3 m_b^2}{32\pi^4} \left(1 - \frac{m_{K^*}^2}{m_B^2}\right)^3 |V_{tb} V_{ts}^* C_7 T_1^{BK^*}(0)|^2, \\ \mathcal{B}(B \rightarrow K_2^* \gamma) &= \tau_B \frac{G_F^2 \alpha_{\text{em}} m_B^5 m_b^2}{256\pi^4 m_{K_2^*}^2} \left(1 - \frac{m_{K_2^*}^2}{m_B^2}\right)^5 |V_{tb} V_{ts}^* C_7 T_1^{BK_2^*}(0)|^2, \end{aligned} \quad (34)$$

with C_7 being the Wilson coefficient for $O_{7\gamma}$ and V_{tb}, V_{ts} being the CKM matrix element. Assuming that C_7 is the same for the above two channels, we obtain the form factors relation

$$\frac{T_1^{BK_2^*}(0)}{T_1^{BK^*}(0)} = (0.52 \pm 0.08), \quad (35)$$

from the experimental data [6]

$$\mathcal{B}(B^- \rightarrow K^{*-}\gamma) = (42.1 \pm 1.8) \times 10^{-6}, \quad \mathcal{B}(B^- \rightarrow K_2^{*-}\gamma) = (14.5 \pm 4.3) \times 10^{-6}. \quad (36)$$

Our result for this ratio, roughly 0.7, is larger than this value but is consistent with it when hadronic uncertainties from the final mesons are taken into account. It also confirms our results that the $B \rightarrow K_2^*$ form factors are smaller than the $B \rightarrow K^*$ ones at $q^2 = 0$ point, in contrast to the LFQM results $T_1^{BK_2^*}(0) \simeq T_1^{BK^*}(0)$ [36].

IV. SEMILEPTONIC $B \rightarrow Tl\bar{\nu}$ DECAYS

Integrating out the off shell W boson, one obtains the effective Hamiltonian responsible for $b \rightarrow ul\bar{\nu}_l$ transition

$$\mathcal{H}_{\text{eff}}(b \rightarrow ul\bar{\nu}_l) = \frac{G_F}{\sqrt{2}} V_{ub} \bar{u} \gamma_\mu (1 - \gamma_5) b \bar{l} \gamma^\mu (1 - \gamma_5) \nu_l, \quad (37)$$

where V_{ub} is the CKM matrix element. In semileptonic $B \rightarrow Tl\bar{\nu}_l$ decays, the helicity of the tensor meson can be $h = 0, \pm 1$ but the $h = 2$ configuration is not allowed physically. Using the form factors obtained in the previous section, we can investigate the semileptonic $B \rightarrow Tl\bar{\nu}$ decays with the partial decay width

$$\begin{aligned} \frac{d\Gamma}{dq^2} &= \sum_{i=L, \pm} \frac{d\Gamma_i}{dq^2}, \\ \frac{d\Gamma_{L, \pm}}{dq^2} &= \frac{|G_F V_{ub}|^2 \sqrt{\lambda_T}}{256 m_B^3 \pi^3 q^2} \left(1 - \frac{m_l^2}{q^2}\right)^2 (X_L, X_\pm) \end{aligned} \quad (38)$$

where $\lambda_T = \lambda(m_B^2, m_T^2, q^2)$, and $\lambda(a^2, b^2, c^2) = (a^2 - b^2 - c^2)^2 - 4b^2c^2$. The subscript (L, \pm) denotes the three polarizations of the tensor meson along its momentum direction: $(0, \pm 1)$. m_l represents the mass of the charged lepton, and q^2 is the momentum square of the lepton pair. In terms of the angular distributions, we can study the forward-backward asymmetries (FBAs) of lepton which are defined as

$$\frac{dA_{FB}}{dq^2} = \frac{\int_0^1 dz (d\Gamma/dq^2 dz) - \int_{-1}^0 dz (d\Gamma/dq^2 dz)}{\int_0^1 dz (d\Gamma/dq^2 dz) + \int_{-1}^0 dz (d\Gamma/dq^2 dz)}$$

where $z = \cos \theta$ and the angle θ is the polar angle of lepton with respect to the moving direction of the tensor meson in the lepton pair rest frame. Explicitly, we have

$$\frac{dA_{FB}}{dq^2} = \frac{1}{X_L + X_+ + X_-} \left(\frac{\lambda_T}{6m_T^2 m_B^2} 2m_l^2 \sqrt{\lambda_T} h_0(q^2) A_0(q^2) - \frac{\lambda_T}{8m_T^2 m_B^2} 4q^4 \sqrt{\lambda_T} A_1(q^2) V(q^2) \right), \quad (39)$$

where

$$\begin{aligned} X_L &= \frac{2}{3} \frac{\lambda_T}{6m_T^2 m_B^2} [(2q^2 + m_l^2) h_0^2(q^2) + 3\lambda_T m_l^2 A_0^2(q^2)], \\ X_\pm &= \frac{2q^2}{3} (2q^2 + m_l^2) \frac{\lambda_T}{8m_T^2 m_B^2} \left[(m_B + m_T) A_1(q^2) \mp \frac{\sqrt{\lambda_T}}{m_B + m_T} V(q^2) \right]^2, \\ h_0(q^2) &= \frac{1}{2m_T} \left[(m_B^2 - m_T^2 - q^2) (m_B + m_T) A_1(q^2) - \frac{\lambda_T}{m_B + m_T} A_2(q^2) \right]. \end{aligned} \quad (40)$$

Integrating over the q^2 , we obtain the partial decay width and integrated angular asymmetry for this decay mode

$$\Gamma = \Gamma_L + \Gamma_+ + \Gamma_-, \quad A_{FB} = \frac{1}{\Gamma} \int dq^2 \int_{-1}^1 \text{sign}(z) dz (d\Gamma/dq^2 dz)$$

with $\Gamma_{L, \pm} = \int_{m_l^2}^{(m_B - m_T)^2} dq^2 \frac{d\Gamma_{L, \pm}}{dq^2}$. Physical quantities \mathcal{B}_L , \mathcal{B}_+ , \mathcal{B}_- , and $\mathcal{B}_{\text{total}}$ can be obtained through different experimental measurements, where $\mathcal{B}_T = \mathcal{B}_+ + \mathcal{B}_-$ and $\mathcal{B}_{\text{total}} = \mathcal{B}_L + \mathcal{B}_T$ with \mathcal{B}_L , \mathcal{B}_+ and \mathcal{B}_- corresponding to

TABLE VI: The branching ratios, polarizations and angular asymmetries for the $b \rightarrow ul\bar{\nu}_l$ ($l = e, \mu$) and $b \rightarrow u\tau\bar{\nu}_\tau$ decay channels (in units of 10^{-4}). \mathcal{B}_L and \mathcal{B}_\pm are the longitudinally and transversely polarized contributions to the branching ratios.

	\mathcal{B}_L	\mathcal{B}_+	\mathcal{B}_-	$\mathcal{B}_{\text{total}}$	f_L	A_{FB}
$\overline{B}^0 \rightarrow a_2^+ l\bar{\nu}_l$	$0.85^{+0.60}_{-0.42}$	~ 0.007	$0.30^{+0.21}_{-0.15}$	$1.16^{+0.81}_{-0.57}$	$73.3^{+0.4}_{-0.5}$	$-0.186^{+0.003}_{-0.002}$
$B^- \rightarrow f_2^0(1270)l\bar{\nu}_l$	$0.52^{+0.36}_{-0.26}$	~ 0.004	$0.17^{+0.11}_{-0.08}$	$0.69^{+0.48}_{-0.34}$	$74.9^{+0.6}_{-0.7}$	-0.175 ± 0.004
$\overline{B}_s \rightarrow K_2^{*+}(1430)l\bar{\nu}_l$	$0.50^{+0.32}_{-0.23}$	~ 0.006	$0.23^{+0.15}_{-0.11}$	$0.73^{+0.48}_{-0.33}$	$68.3^{+0.5}_{-0.5}$	-0.221 ± 0.005
$\overline{B}^0 \rightarrow a_2^+ \tau\bar{\nu}_\tau$	$0.29^{+0.20}_{-0.14}$	~ 0.004	$0.12^{+0.08}_{-0.06}$	$0.41^{+0.29}_{-0.20}$	$69.9^{+0.6}_{-0.6}$	0.031 ± 0.005
$B^- \rightarrow f_2^0(1270)\tau\bar{\nu}_\tau$	$0.18^{+0.13}_{-0.09}$	~ 0.002	$0.07^{+0.05}_{-0.03}$	$0.25^{+0.18}_{-0.13}$	$71.9^{+0.8}_{-0.8}$	0.048 ± 0.007
$\overline{B}_s \rightarrow K_2^{*+}(1430)\tau\bar{\nu}_\tau$	$0.16^{+0.10}_{-0.07}$	~ 0.003	$0.09^{+0.06}_{-0.04}$	$0.25^{+0.17}_{-0.12}$	$64.1^{+0.4}_{-0.3}$	-0.024 ± 0.005

contributions of different polarization configurations to branching ratios. Since there are three different polarizations, it is also meaningful to define the polarization fraction

$$f_L = \frac{\Gamma_L}{\Gamma_L + \Gamma_+ + \Gamma_-}. \quad (41)$$

Our theoretical results for the $B \rightarrow Tl\bar{\nu}_l$ ($l = e, \mu$) and $B \rightarrow T\tau\bar{\nu}_\tau$ decays are listed in Table VI, with masses of the electron and muon neglected in the case of $l = e, \mu$. The B meson lifetime is taken from the particle data group and the CKM matrix element V_{ub} is employed as $|V_{ub}| = (3.89 \pm 0.44) \times 10^{-3}$ [1].

Some remarks are given in order.

- Most of the total branching ratios are of the order 10^{-4} , implying a promising prospect to measure these channels at the Super B factories and the LHCb. A tensor meson can be reconstructed in the final state of two or three pseudoscalar mesons.
- The heavy τ lepton will bring a smaller phase space than the lighter electron, thus the branching ratios of $B \rightarrow T\tau\bar{\nu}_\tau$ decays are smaller than those of the corresponding $B \rightarrow Te\bar{\nu}_e$ decay modes by a factor of 3.
- The positively polarized branching ratio Br_+ is tiny since the A_1 term cancels with the contribution from V . The longitudinal contributions are about twice as large as the transverse polarizations and accordingly the polarization fraction f_L is around (60% – 70%)
- For $l = (e, \mu)$ the angular asymmetries are negative since only the second terms in Eq. (39) contribute. In the case of $l = \tau$, the two terms give destructive contributions, resulting in tiny angular asymmetries in magnitude.
- In the polarization fractions and angular asymmetries, the uncertainties from the form factors and the CKM matrix element will mostly cancel and thus they are stable against hadronic uncertainties.

V. SUMMARY

Inspired by the success of the PQCD approach in the application to B decays into s-wave mesons, we give a comprehensive study on the $B \rightarrow T$ transition form factors. Our results will become necessary inputs in the analysis of the nonleptonic B decays into a tensor meson.

The similarities in the Lorentz structures of the wave functions and B decay form factors involving a vector and a tensor meson allow us to obtain the factorization formulas of $B \rightarrow T$ form factors from the $B \rightarrow V$ ones. Furthermore, the light-cone distribution amplitudes of tensor mesons and vector mesons have similar shapes in the dominant region of the perturbative QCD approach, and thus these two sets of form factors are found to have the same signs and related q^2 -dependence behaviors. In the large recoil region, we find that our results for the form factors satisfy the relations derived from the large energy limit. The two independent functions ζ_\perp and ζ_\parallel are found to have similar size at $q^2 = 0$ point. We also find that the $B \rightarrow T$ form factors are smaller than the $B \rightarrow V$ ones, which is supported by the experimental data of radiative B decays.

At last, we also use these results to explore semileptonic $B \rightarrow Tl\bar{\nu}_l$ decays and we find that the branching fractions can reach the order 10^{-4} , implying a promising prospect to observe these channels.

Acknowledgements

I would like to acknowledge Hai-Yang Cheng and Ying Li for useful discussions. I am very grateful to Pietro Colangelo and Fulvia De Fazio for their warm hospitality during my stay in Bari. This work is supported by the INFN through the program of INFN fellowship for foreigners and also in part by the National Natural Science Foundation of China under the Grant No. 10805037 and 10947007.

-
- [1] K. Nakamura *et al.* [Particle Data Group], J. Phys. G **37**, 075021 (2010).
 - [2] B. Aubert *et al.* [BABAR Collaboration], Phys. Rev. Lett. **97**, 201802 (2006) [arXiv:hep-ex/0608005].
 - [3] B. Aubert *et al.* [BABAR Collaboration], Phys. Rev. D **79**, 052005 (2009) [arXiv:0901.3703 [hep-ex]].
 - [4] B. Aubert *et al.* [BABAR Collaboration], Phys. Rev. Lett. **101**, 161801 (2008) [arXiv:0806.4419 [hep-ex]].
 - [5] B. Aubert *et al.* [The BABAR Collaboration], Phys. Rev. D **78**, 092008 (2008) [arXiv:0808.3586 [hep-ex]].
 - [6] E. Barberio *et al.* [Heavy Flavor Averaging Group (HFAG)], arXiv:0808.1297. The updated results can be found at www.slac.stanford.edu/xorg/hfag.
 - [7] Y. Y. Keum, H. n. Li and A. I. Sanda, Phys. Lett. B **504**, 6 (2001) [arXiv:hep-ph/0004004]; Phys. Rev. D **63**, 054008 (2001) [arXiv:hep-ph/0004173]; C. D. Lu, K. Ukai and M. Z. Yang, Phys. Rev. D **63**, 074009 (2001) [arXiv:hep-ph/0004213].
 - [8] H. Y. Cheng, Y. Koike and K. C. Yang, Phys. Rev. D **82**, 054019 (2010) [arXiv:1007.3541 [hep-ph]].
 - [9] T. M. Aliev and M. A. Shifman, Phys. Lett. B **112**, 401 (1982).
 - [10] T. M. Aliev and M. A. Shifman, Sov. J. Nucl. Phys. **36** (1982) 891 [Yad. Fiz. **36** (1982) 1532].
 - [11] T. M. Aliev, K. Azizi and V. Bashiry, J. Phys. G **37**, 025001 (2010) [arXiv:0909.2412 [hep-ph]].
 - [12] C. Allton *et al.* [RBC-UKQCD Collaboration], Phys. Rev. D **78**, 114509 (2008) [arXiv:0804.0473 [hep-lat]].
 - [13] T. Kurimoto, H. n. Li and A. I. Sanda, Phys. Rev. D **65**, 014007 (2002) [arXiv:hep-ph/0105003]; Z. T. Wei and M. Z. Yang, Nucl. Phys. B **642**, 263 (2002) [arXiv:hep-ph/0202018]; C. D. Lu and M. Z. Yang, Eur. Phys. J. C **28**, 515 (2003) [arXiv:hep-ph/0212373].
 - [14] A. Ali, *et al.*, Phys. Rev. D **76**, 074018 (2007) [arXiv:hep-ph/0703162].
 - [15] E. Gamiz, C. T. H. Davies, G. P. Lepage, J. Shigemitsu and M. Wingate [HPQCD Collaboration], Phys. Rev. D **80**, 014503 (2009) [arXiv:0902.1815 [hep-lat]].
 - [16] H. n. Li and H. L. Yu, Phys. Rev. D **53**, 2480 (1996) [arXiv:hep-ph/9411308].
 - [17] H. n. Li, Phys. Rev. D **66**, 094010 (2002) [arXiv:hep-ph/0102013]; H. n. Li and K. Ukai, Phys. Lett. B **555**, 197 (2003) [arXiv:hep-ph/0211272].
 - [18] H. n. Li, Prog. Part. Nucl. Phys. **51**, 85 (2003) [arXiv:hep-ph/0303116].
 - [19] C. H. Chen and C. Q. Geng, Nucl. Phys. B **636**, 338 (2002) [arXiv:hep-ph/0203003].
 - [20] W. Wang, Y. L. Shen, Y. Li and C. D. Lu, Phys. Rev. D **74**, 114010 (2006) [arXiv:hep-ph/0609082].
 - [21] R. H. Li, C. D. Lu, W. Wang and X. X. Wang, Phys. Rev. D **79**, 014013 (2009) [arXiv:0811.2648 [hep-ph]] .
 - [22] W. Wang, R. H. Li and C. D. Lu, arXiv:0711.0432 [hep-ph].
 - [23] R. H. Li, C. D. Lu and W. Wang, Phys. Rev. D **79**, 034014 (2009) [arXiv:0901.0307 [hep-ph]].
 - [24] T. Kurimoto, H. n. Li and A. I. Sanda, Phys. Rev. D **67**, 054028 (2003) [arXiv:hep-ph/0210289].
 - [25] R. H. Li, C. D. Lu and H. Zou, Phys. Rev. D **78**, 014018 (2008) [arXiv:0803.1073 [hep-ph]].
 - [26] N. Isgur, D. Scora, B. Grinstein and M. B. Wise, Phys. Rev. D **39**, 799 (1989).
 - [27] D. Becirevic and A. B. Kaidalov, Phys. Lett. B **478**, 417 (2000) [arXiv:hep-ph/9904490].
 - [28] P. Ball, V. M. Braun and A. Lenz, JHEP **0605**, 004 (2006) [arXiv:hep-ph/0603063]; P. Ball and G. W. Jones, JHEP **0703**, 069 (2007) [arXiv:hep-ph/0702100].
 - [29] C. H. Chen, Y. Y. Keum and H. n. Li, Phys. Rev. D **64**, 112002 (2001) [arXiv:hep-ph/0107165].
 - [30] D. Scora and N. Isgur, Phys. Rev. D **52**, 2783 (1995) [arXiv:hep-ph/9503486].
 - [31] C. S. Kim, J. P. Lee and S. Oh, Phys. Rev. D **67**, 014002 (2003) [arXiv:hep-ph/0205263].
 - [32] N. Sharma and R. C. Verma, arXiv:1004.1928 [hep-ph].
 - [33] H. Y. Cheng and C. K. Chua, Phys. Rev. D **82**, 034014 (2010) [arXiv:1005.1968 [hep-ph]].
 - [34] H. Y. Cheng, C. K. Chua and C. W. Hwang, Phys. Rev. D **69**, 074025 (2004) [arXiv:hep-ph/0310359].
 - [35] H. Y. Cheng and C. K. Chua, Phys. Rev. D **69**, 094007 (2004) [Erratum-ibid. D **81**, 059901 (2010)] [arXiv:hep-ph/0401141].
 - [36] H. Y. Cheng and C. K. Chua, Phys. Rev. D **81**, 114006 (2010) [arXiv:0909.4627 [hep-ph]].
 - [37] A. S. Safir, Eur. Phys. J. direct C **3**, 15 (2001) [arXiv:hep-ph/0109232].
 - [38] D. Ebert, R. N. Faustov, V. O. Galkin and H. Toki, Phys. Rev. D **64**, 054001 (2001) [arXiv:hep-ph/0104264].
 - [39] S. Veseli and M. G. Olsson, Phys. Lett. B **367**, 309 (1996) [arXiv:hep-ph/9508255].
 - [40] A. Datta, *et al.*, Phys. Rev. D **77**, 114025 (2008) [arXiv:0711.2107 [hep-ph]].
 - [41] H. Hatanaka and K. C. Yang, Phys. Rev. D **79**, 114008 (2009) [arXiv:0903.1917 [hep-ph]]; Eur. Phys. J. C **67**, 149 (2010) [arXiv:0907.1496 [hep-ph]].